Available online at www.sciencedirect.com
SCIENCE DIRECT®
Journal of Sound and Vibration 283 (2005) 981–996
JOURNAL OF SOUND AND VIBRATION
www.elsevier.com/locate/jsvi

# Semi-active $H_\infty$ control of vehicle suspension with magneto-rheological dampers

Haiping Du[a,*], Kam Yim Sze[b], James Lam[b]

[a]*Control and Power Group, Electrical and Electronic Engineering Department, Imperial College, Exhibition Road, London SW7 2BT, UK*
[b]*Department of Mechanical Engineering, University of Hong Kong, Pokfulam Road, Hong Kong*

Received 14 October 2003; received in revised form 18 May 2004; accepted 26 May 2004

**Abstract**

Semi-active $H_\infty$ control of vehicle suspension with magneto-rheological (MR) damper is studied in this paper. First, an experiment is conducted on an MR damper prototype subjected to cyclic excitation. Then, a polynomial model is adopted to characterize the dynamic response of the MR damper. Such a model has an advantage that it can represent the inverse dynamics of the MR damper analytically, so that the desired output in the open-loop control scheme can be realized easily. Finally, a static output feedback $H_\infty$ controller which utilizes the measurable suspension deflection and sprung mass velocity as feedback signals for active vehicle suspension is designed. The active control force is realized with the MR damper using the obtained polynomial model. A quarter-car suspension model is considered in this paper for analysis and simulation. The proposed scheme is further validated by numerical simulation under random excitation. Simulation results showed that the designed static output feedback $H_\infty$ controller realized by the MR damper can achieve good active suspension performance.


## 1. Introduction

There are three main types of vehicle suspensions that have been proposed, that is, passive, semi-active and active suspensions, which depend on the operation mode to improve vehicle ride

*Corresponding author.
*E-mail address:* h.du@imperial.ac.uk (H. Du).

0022-460X/$ - see front matter © 2004 Elsevier Ltd. All rights reserved.
doi:10.1016/j.jsv.2004.05.030

comfort, vehicle safety, road damage minimization and the overall vehicle performance. Normally, conventional passive suspensions are effective only in a certain frequency range and no on-line feedback action is used. Thus, optimal design performance cannot be achieved when the system and its operating conditions are changed. On the contrary, active suspensions can improve the performance of the suspension systems over a wide range of frequency and can adapt to the system variations based on on-line changes of the actuating force. Therefore, active suspensions have been extensively studied since 1960s and various approaches have been proposed, see Ref. [1] and references therein. However, active suspensions normally require large power supply, which is the main drawback that prevents this technique from being used extensively in practice. Since 1970s, semi-active suspensions have received much attention since they can achieve desirable performance than passive suspensions and consume much less power than that of active suspensions. Especially, when some controllable dampers, such as electro-rheological (ER) dampers and magneto-rheological (MR) dampers, are available in practice recently, semi-active suspensions are more practical than ever in engineering realization.

In particular, MR dampers have found considerable attraction in vibration reduction of bridges, helicopter rotors, truss structures, suspension seats, seismic reduction, and vibration isolator, etc. Semi-active control with MR dampers for vehicle suspensions have also been studied by many researchers [2,3]. Many control strategies such as skyhook, groundhook and hybrid control [4], $H_\infty$ control [5] and model-following sliding mode control [6] have been evaluated in terms of their applicability in practice.

However, the practical use of MR dampers for control is significantly hindered by its inherently hysteretic and highly nonlinear dynamics. This makes the modeling of MR dampers very important for its application. In order to characterize the performance of MR dampers, several models have been proposed to describe their behavior. These include the phenomenological model based on a Bouc–Wen hysteresis model proposed by Spencer et al. [7], neural network model developed by Chang and Roschke [8,9], fuzzy model [10], nonlinear blackbox model [11], NARX model [12], viscoelastic–plastic model [13], polynomial model [14] and other approaches [15]. Among these MR models, phenomenological model and viscoelastic–plastic model can accurately describe the behavior of the MR dampers, but the corresponding models for the inverse dynamics of the MR dampers are often difficult to obtain due to their nonlinear characteristics. Neural network and fuzzy models can be used to emulate the inverse dynamics of the MR dampers, but the selection of network structure and training data are essential in order to obtain accurate results. In fact, the polynomial model is a convenient and effective choice which can realize the inverse dynamics of the MR damper in an analytical form, and is easy to achieve the desirable damper force in an open-loop control system. A shortcoming of polynomial models is that it cannot characterize the MR behavior favorably at relatively low velocity region since the model does not include variables characterizing the pre-yield property of the damper force.

In addition, theoretical and experimental researches have demonstrated that the performance of a semi-active control system is also highly dependent on the choice of control strategy [16]. Therefore, some semi-active control schemes have been presented and compared in Ref. [17] and many other approaches, such as neuro-fuzzy control [18], and observer-based control [19], are also incorporated into the semi-active control.

It can be concluded that the success of MR dampers in semi-active vehicle suspension applications is determined by two aspects: one is the accurate modeling of the MR dampers and

the other is the selection of an appropriate control strategy. The latter is often related to the selection of a model for an MR damper. Based on previous research results, this paper is mainly concerned with semi-active static output feedback $H_\infty$ control with MR dampers for vehicle suspension systems. A polynomial model is used here to model the MR damper using experimental data. Using this model, the damper force is mainly dependent upon the velocity of damper motion and input current. If the desired damper force is given and the damper motion velocity is measured, the input current can be calculated according to this model. Therefore, the desired damper force can be accurately tracked in the open-loop control system. In order to utilize this model sufficiently and to meet the three main performance requirements for advanced vehicle suspensions (ride comfort, road holding, and suspension deflection), an appropriate static output feedback $H_\infty$ controller, which utilizes the measurable suspension deflection and sprung mass velocity as feedback signals, is designed to provide a trade-off between these requirements. A quarter-car suspension model is used here to study the performance of a vehicle suspension system in terms of the bouncing motion, the tyre deflection, and other performance features. The research of this paper is different from the recent research results [2,3] in that (a) a polynomial model is used, (b) a static output feedback $H_\infty$ controller is designed to fit to this model and, (c) no closed-loop control system is required to make the actual damper force tracks the desired damper force. The performance of the presented scheme is further evaluated by computer simulation under random excitation in time domain. It is demonstrated via simulation results that the designed semi-active vehicle suspension can achieve good performance imitating that of active suspension.

The rest of this paper is organized as follows. Section 2 presents a description of the experiment and modeling of the MR damper. A quarter-car suspension model and the formulation of the static output feedback $H_\infty$ controller design problem are presented in Section 3. Section 4 presents the design results and performance evaluations. Conclusions are given in Section 5.

## 2. Experiment and modeling of MR damper

### 2.1. Experimental setup and results

To evaluate the potential application of MR dampers in vibration control of vehicle suspension system, a model is developed to accurately reproduce the behavior of the MR damper and an experiment is set up to obtain the dynamic data necessary for identifying its model parameters.

The prototype MR damper used in this study is RD-1005-3, which was manufactured by Lord Corporation. The length of the damper is 208 mm in its extended position. It has a $\pm 25$ mm stroke. The maximum input current to the electromagnet in the magnetic is 2 A and the coil resistance at ambient temperature is $5\,\Omega$.

The MR damper is tested by using the MTS810 TestStar Material Testing System, shown in Fig. 1. The MTS810 test machine has an upper and lower head with grippers that can hold the dampers in place. The lower head is attached to the hydraulic cylinder that can move up and down. The upper head incorporates a load cell allowing the operator to measure the force applied to the MR damper.

The MR damper is first mounted in position by the grippers, preliminary tests are then conducted to measure the response of the damper under various loading conditions. In each test,

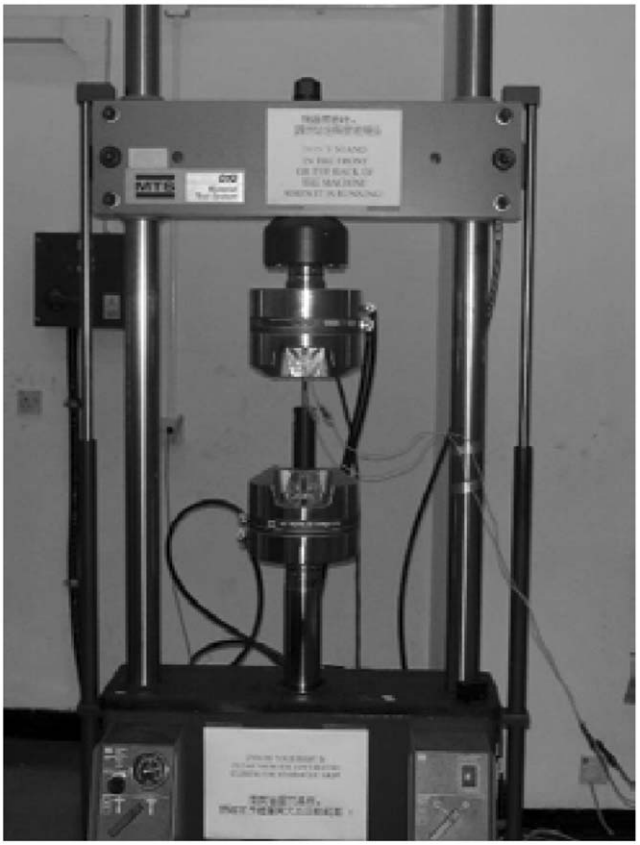

Fig. 1. MTS 810 TestStar Material Testing System.

the hydraulic actuator drives the lower head with a sinusoidally varying displacement of fixed frequency and constant amplitude, and the input current to the MR damper is maintained at constant level, while the upper head is held fixed. The excitation frequencies are 0.05, 0.1, 0.2, 0.5, 1 and 2 Hz and the displacement amplitudes are 2.5, 5, 10 and 15 mm, respectively. The applied input current is from 0 to 1 A with increments of 0.25 A. The damper force is measured and fed to a personal computer. Velocity is obtained by differentiating the displacement.

For brevity, only the responses of the MR damper at 1 Hz and 15 mm excitation under five different input currents are shown in Figs. 2(a) and (b). It can be seen that with the increase of the input current, the damper force will markedly increase when the input current is less than 0.75 A. It is also noted that the damper force is not exactly centered at zero due to the presence of an accumulation in the MR damper.

### 2.2. Polynomial model

The polynomial model proposed by Choi et al. [14] is adopted in this study for the MR damper using the obtained experimental data. In this model, the hysteresis loop of the MR damper is

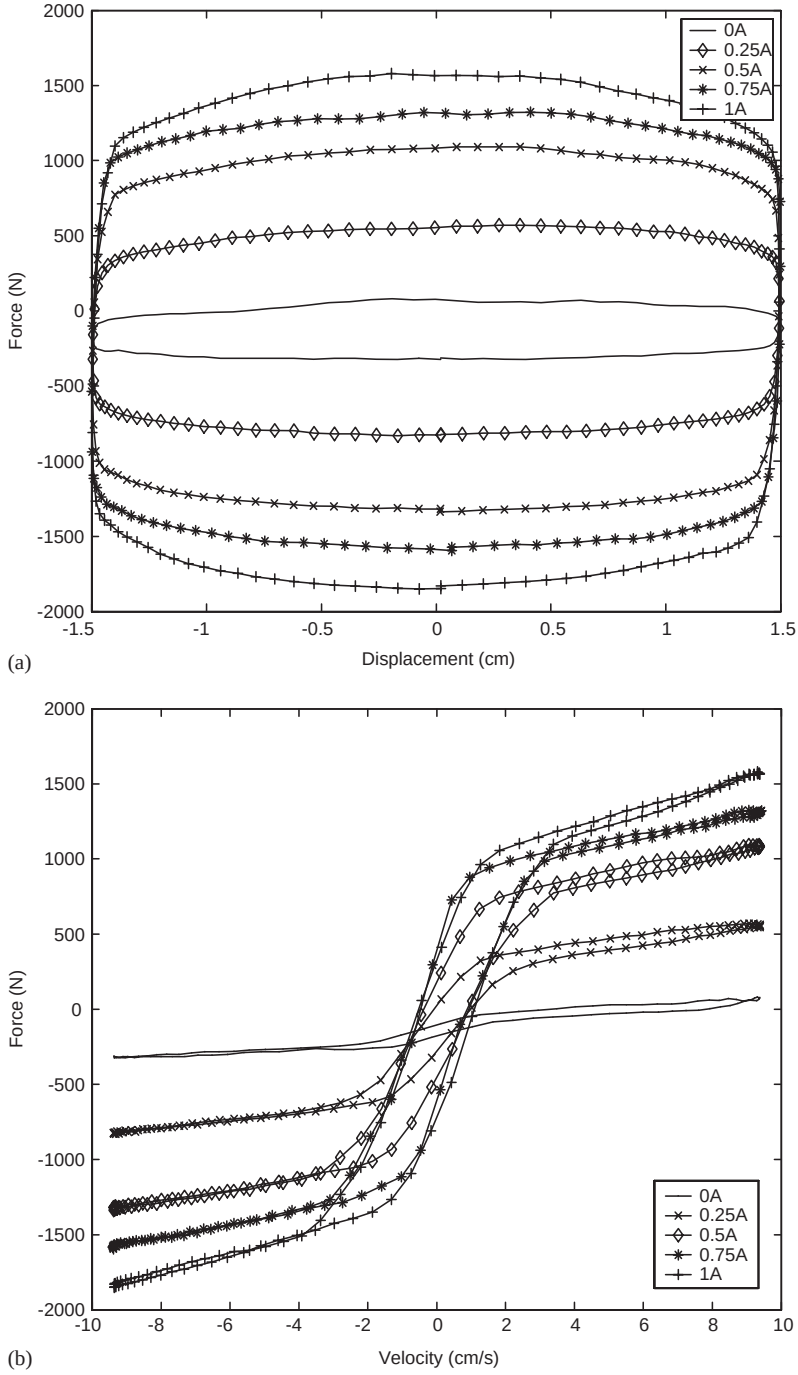


Fig. 2. Experimental results (1 Hz, ±15 mm): (a) force vs. displacement; (b) force vs. velocity.

divided into positive acceleration (lower loop) and negative acceleration (upper loop), and the lower loop or the upper loop is fitted by the polynomial with the power of the damper piston velocity as follows:

$$F = \sum_{i=0}^{n} a_i v^i, \tag{1}$$

where $F$ is the damper force, $a_i$ is the experimental coefficient to be determined from the curve fitting, $v$ is the damper piston velocity. The polynomial order $n$ is chosen by trial and error. Based on the experimental data, a least-square optimization method is employed to determine the appropriate parameters $a_i$ and $n$ for the analytical model. In this work, $n = 11$ is selected.

The coefficient $a_i$ in Eq. (1) can be further expressed with respect to the input current as shown in Fig. 3 for $a_0$ and $a_2$ (the other coefficients are omitted for brevity).

It can be observed that the coefficient $a_i$ can be linearly approximated with respect to the input current as follows:

$$a_i = b_i + c_i I, \quad i = 0, 1, \ldots, 11. \tag{2}$$

Therefore, the damper force is further represented by

$$F = \sum_{i=0}^{n} (b_i + c_i I) v^i, \tag{3}$$

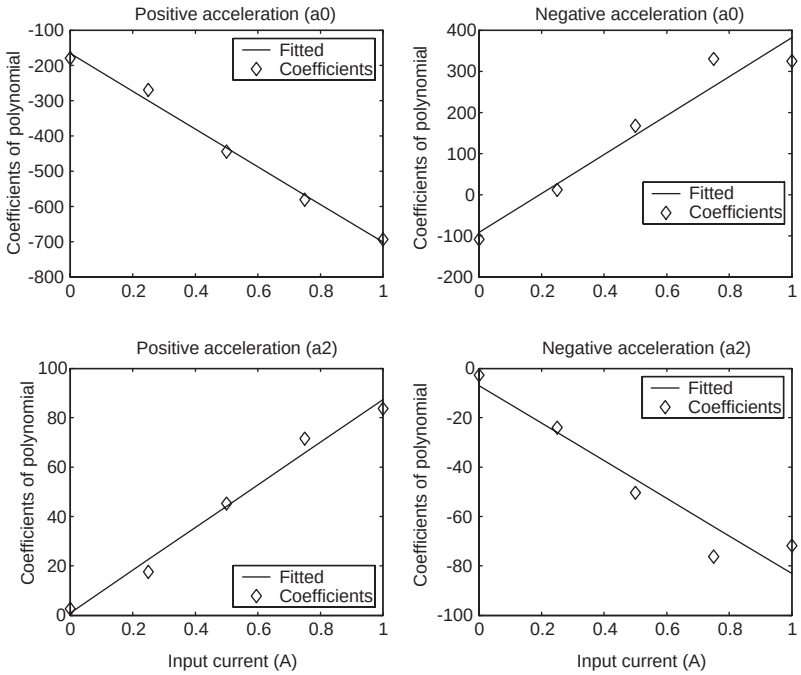


Fig. 3. The relationship between $a_i, i = 0, 2$, and input current.

Table 1
Coefficients $b_i$ and $c_i$ of the polynomial model

| Positive acceleration | | | | Negative acceleration | | | |
|---|---|---|---|---|---|---|---|
| Coefficients | | Coefficients | | Coefficients | | Coefficients | |
| $b_0$ | $-165.66$ | $c_0$ | $-535.57$ | $b_0$ | $-91.80$ | $c_0$ | 473.89 |
| $b_1$ | 114.63 | $c_1$ | 530.84 | $b_1$ | 121.49 | $c_1$ | 560.46 |
| $b_2$ | 0.85 | $c_2$ | 86.52 | $b_2$ | $-6.95$ | $c_2$ | $-76.17$ |
| $b_3$ | $-7.39$ | $c_3$ | $-21.73$ | $b_3$ | $-7.06$ | $c_3$ | $-26.41$ |
| $b_4$ | $-0.02$ | $c_4$ | $-4.69$ | $b_4$ | 0.45 | $c_4$ | 4.01 |
| $b_5$ | 0.29 | $c_5$ | 0.64 | $b_5$ | 0.26 | $c_5$ | 0.89 |
| $b_6$ | $-8.16\times10^{-6}$ | $c_6$ | 0.11 | $b_6$ | $-0.01$ | $c_6$ | $-0.09$ |
| $b_7$ | $-5.9\times10^{-3}$ | $c_7$ | $-0.01$ | $b_7$ | $-5.1\times10^{-3}$ | $c_7$ | $-0.02$ |
| $b_8$ | $5.15\times10^{-6}$ | $c_8$ | $-1.2\times10^{-3}$ | $b_8$ | $1.34\times10^{-4}$ | $c_8$ | $9.98\times10^{-4}$ |
| $b_9$ | $5.65\times10^{-5}$ | $c_9$ | $8.34\times10^{-5}$ | $b_9$ | $4.71\times10^{-5}$ | $c_9$ | $1.49\times10^{-4}$ |
| $b_{10}$ | $-3.37\times10^{-8}$ | $c_{10}$ | $4.63\times10^{-6}$ | $b_{10}$ | $-5.51\times10^{-7}$ | $c_{10}$ | $-3.96\times10^{-6}$ |
| $b_{11}$ | $-2.05\times10^{-7}$ | $c_{11}$ | $-2.69\times10^{-7}$ | $b_{11}$ | $-1.68\times10^{-7}$ | $c_{11}$ | $-5.32\times10^{-7}$ |

where the coefficients $b_i$ and $c_i$ are obtained from the fitness of data in the plots. The specific values of $b_i$ and $c_i$ used in this work are listed in Table 1.

In order to validate the obtained polynomial model, the measured damper force and the predicted damper force obtained from the polynomial model are compared as shown in Figs. 4(a) and (b), where the excitation frequency and amplitude are selected as 1 Hz and $\pm15$ mm, respectively. It is clearly observed that the measured damper force is well predicted by the polynomial model. To check generally the effectiveness of the polynomial model, the excitation conditions and the input current are changed. By comparing the results between the measurement and the simulation under various operating conditions, it can be concluded that the polynomial model predicts the damper force well under various conditions without modifying the coefficients of $a_i$, $b_i$ and $c_i$.

Once the polynomial model is determined, the desirable damper force can be realized by injecting an appropriate current into the MR damper in accordance with the piston velocity of the MR damper. This input current is calculated from Eq. (3) with measurable velocity $v$ and is given by

$$I = \frac{F_d - \sum_{i=0}^{n} b_i v^i}{\sum_{i=0}^{n} c_i v^i}, \tag{4}$$

where $I$ is the input current to the MR damper, $F_d$ is the desired damper force to be tracked. The desired damper force is often designed by an appropriate controller in practice. It should be noted that the MR damper is a passive device and the current sent to the MR damper should be restricted in the range of zero and the maximum value. Therefore, although the desired force can be any value, the calculated current using Eq. (4) should be constrained.

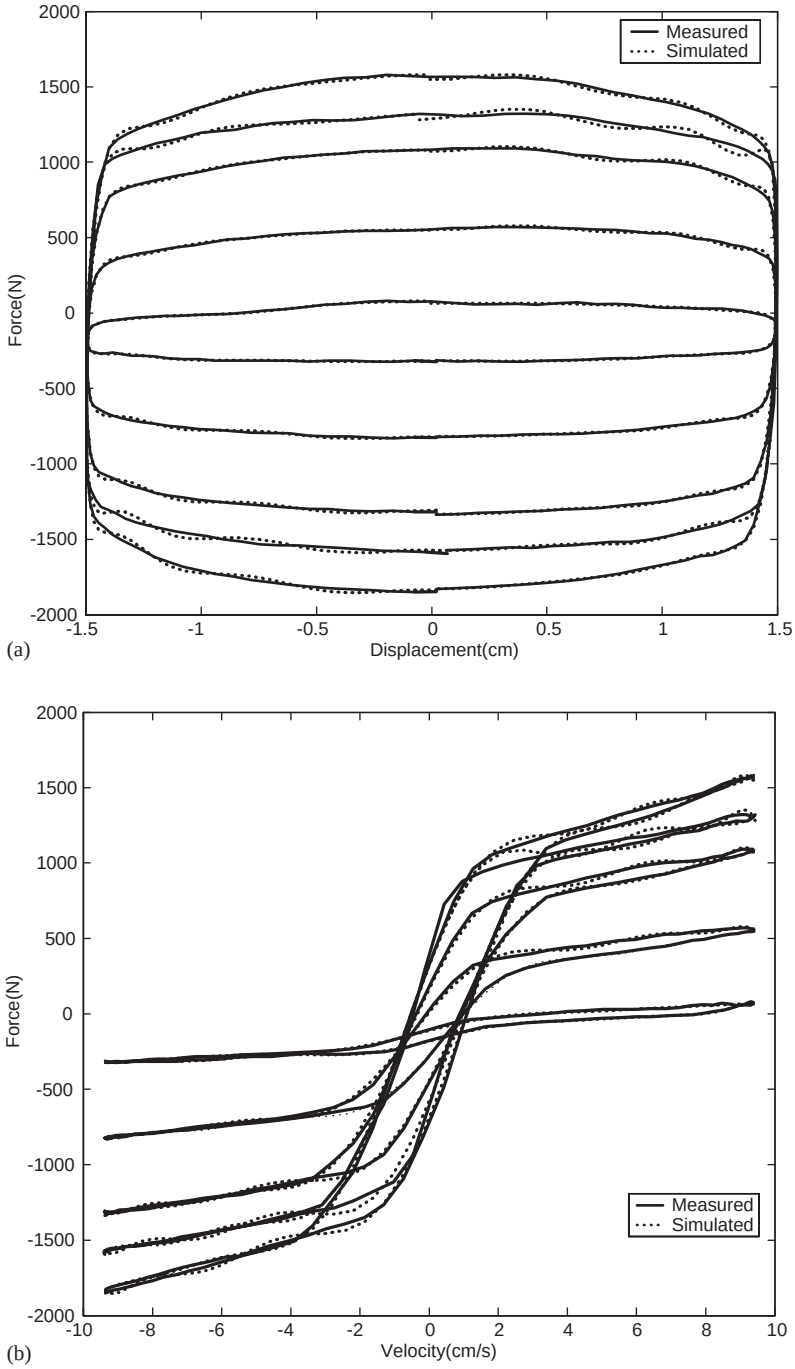


Fig. 4. Comparison of polynomial model and experimental results (1 Hz, ±15 mm): (a) force vs. displacement; (b) force vs. velocity.

## 3. Static output $H_\infty$ control of vehicle suspension system

### 3.1. Vehicle suspension model

In this study, a simple quarter-car suspension model that consists of one-fourth of the body mass, suspension components and one wheel is shown in Fig. 5. This model has been used extensively in the literature and captures many essential characteristics of a real suspension system. The equations of motion for the sprung and unsprung masses of the quarter-car suspension model are given by

$$m_s\ddot{z}_s(t) + c_s[\dot{z}_s(t) - \dot{z}_u(t)] + k_s[z_s(t) - z_u(t)] = -u(t), \tag{5}$$

$$m_u\ddot{z}_u(t) + c_s[\dot{z}_u(t) - \dot{z}_s(t)] + k_s[z_u(t) - z_s(t)] + k_t[z_u(t) - z_r(t)] = u(t), \tag{6}$$

where $m_s$ is the sprung mass, which represents the car chassis; $m_u$ is the unsprung mass, which represents the wheel assembly; $c_s$ and $k_s$ are damping and stiffness of the uncontrolled suspension system, respectively; $k_t$ serves to model the compressibility of the pneumatic tyre; $z_s(t)$ and $z_u(t)$ are the displacements of the sprung and unsprung masses, respectively; $z_r(t)$ is the road displacement input; $u(t)$ represents the external input force of the suspension system. This input force can be generated by means of a hydraulic actuator placed between the two masses [20] for active control or by means of a MR damper for semi-active control [2].

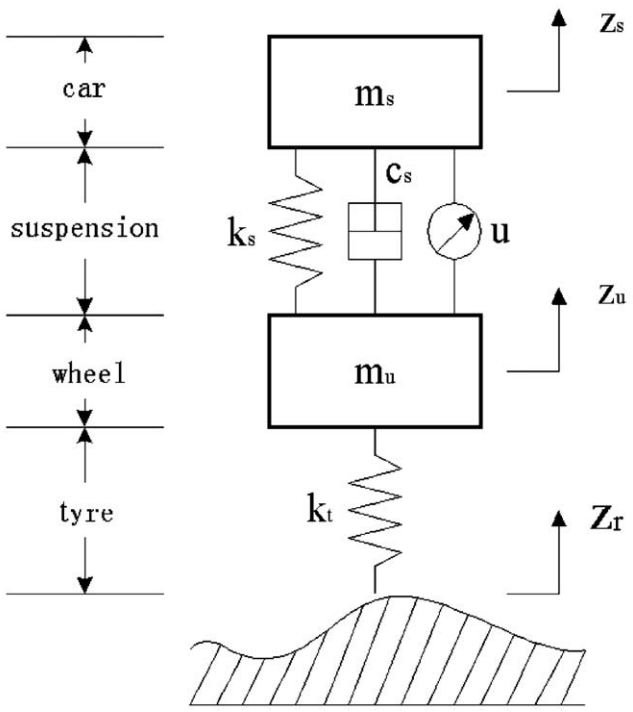


Fig. 5. Quarter-car suspension model.

After choosing the state variables as

$$x_1(t) = z_s(t) - z_u(t), \quad x_2(t) = z_u(t) - z_r(t), \quad x_3(t) = \dot{z}_s(t), \quad x_4(t) = \dot{z}_u(t), \tag{7}$$

where $x_1(t)$ denotes the suspension deflection, $x_2(t)$ is the tyre deflection, $x_3(t)$ is the sprung mass speed, $x_4(t)$ denotes the unsprung mass speed, and defining

$$x(t) = \begin{bmatrix} x_1(t) & x_2(t) & x_3(t) & x_4(t) \end{bmatrix}^{\mathrm{T}}, \quad w(t) = \dot{z}_r(t), \tag{8}$$

where $w(t)$ represents the disturbance caused by road roughness, Eqs. (5)–(6) can be written in state-space form as

$$\dot{x}(t) = Ax(t) + Bu(t) + B_w w(t), \tag{9}$$

where

$$A = \begin{bmatrix} 0 & 0 & 1 & -1 \\ 0 & 0 & 0 & 1 \\ -k_s/m_s & 0 & -c_s/m_s & c_s/m_s \\ k_s/m_u & -k_t/m_s & c_s/m_s & -c_s/m_s \end{bmatrix}, \quad B = \begin{bmatrix} 0 \\ 0 \\ -1/m_s \\ 1/m_u \end{bmatrix}, \quad B_w = \begin{bmatrix} 0 \\ -1 \\ 0 \\ 0 \end{bmatrix},$$

are constant matrices.

### 3.2. Formulation of static output $H_\infty$ controller

Ride comfort, road holding ability and suspension deflection are three main performance criteria in vehicle suspension design. It is widely accepted that ride comfort is closely related to the vertical acceleration experienced by the car body. Consequently, to improve ride comfort amounts to keep the transfer characteristics from road disturbance to car body (sprung mass) acceleration small over the frequency range of 0–65 rad/s [21]. Due to the disturbances caused by road bumpiness, a firm uninterrupted contact of wheels to road (good road holding) is important for vehicle handling and is essentially related to driving safety. To ensure good road holding, it is required that the transfer function from road disturbance to tyre deflection $z_u(t) - z_r(t)$ should be small. The structural features of the vehicle also constrains the amount of suspension deflection $z_s(t) - z_u(t)$ with a hard limit. Hitting the deflection limit not only results in the rapid deterioration on the ride comfort, but at the same time increases the wear of the suspension system. Hence, it is also important to keep the transfer function from road disturbance to suspension deflection $z_s(t) - z_u(t)$ small enough to prevent excessive suspension bottoming.

In accordance with the aforementioned requirements, we formulate an $H_\infty$ control problem to deal with the three different objectives for vehicle suspension. It is standard in the $H_\infty$ framework to use weighting functions to shape and compromise different performance objectives. In order to satisfy the performance requirement, we define the controlled output $z(t)$ as $\ddot{z}_s(t)$, $z_s(t) - z_u(t)$, and $z_u(t) - z_r(t)$, respectively, for the quarter-car suspension model. We consider the case that only the suspension deflection $z_s(t) - z_u(t)$ and the velocity of sprung mass $\dot{z}_s(t)$ are measurable. (In practice, the suspension deflection can be measured by acoustic or radar transmitter/receiver; while the velocity is typically obtained by integrating the acceleration which is measured using accelerometer [22].) That is, we need to consider the design of a static output feedback $H_\infty$ controller.

Given the system described by equations of the form

$$\begin{aligned} \dot{x}(t) &= Ax(t) + Bu(t) + B_w w(t), \\ z(t) &= C_1 x(t) + D_1 u(t), \\ y(t) &= C_2 x(t), \end{aligned} \tag{10}$$

where $x(t)$, $w(t)$, $A$, $B$, $B_w$ are defined as in Eq. (9) and

$$C_1 = \begin{bmatrix} -k_s/m_s & 0 & -c_s/m_s & c_s/m_s \\ \alpha & 0 & 0 & 0 \\ 0 & \beta & 0 & 0 \end{bmatrix}, \quad D_1 = \begin{bmatrix} -1/m_s & 0 & 0 \end{bmatrix}^{\mathrm{T}}, \tag{11}$$

where $\alpha > 0$ and $\beta > 0$ are scalar weightings for the suspension deflection and tyre deflection, respectively. These weightings are used to control the trade-off between the control objectives. The control signals are the suspension deflection and the velocity of the sprung mass so that

$$C_2 = \begin{bmatrix} 1 & 0 & 0 & 0 \\ 0 & 0 & 1 & 0 \end{bmatrix}.$$

We formulate the following static output feedback $H_\infty$ control problem for vehicle suspension as finding a static output feedback controller of the following form:

$$u(t) = Ky(t) = KC_2 x(t), \tag{12}$$

where $K = \begin{bmatrix} k_1, & k_2 \end{bmatrix}$ is the output feedback gain matrix to be designed such that

1. the resulting closed-loop system is asymptotically stable, and
2. the $H_\infty$-norm of the closed-loop transfer function matrix $T_{zw}(s, K)$ from $w$ to $z$, denoted by $||T_{zw}(s, K)||_\infty$, is bounded by a constant $\gamma > 0$.

Although output feedback controller designs involving fixed order or static gain can be computationally demanding [23], the parameter matrix $K$ in this problem can be designed by using genetic algorithms (GAs) [24] via the following minimization problem:

$$\min_{K \in \mathscr{S}_K} \left\| T_{zw}(s; K) \right\|_\infty,$$

where $\mathscr{S}_K \triangleq \{K \mid T_{zw}(s; K) \text{ is stable}\}$. The computation procedure is similar as that used in Ref. [24] and omitted here for brevity.

## 4. Simulation results

In this section, the performance of the semi-active static output feedback $H_\infty$ controller applied to the quarter-car suspension model with MR damper is evaluated. The quarter-car suspension model parameters have the following values [25]:

$$m_s = 504.5\,\mathrm{kg}, \quad m_u = 62\,\mathrm{kg}, \quad k_s = 13\,100\,\mathrm{N/m}, \quad c_s = 400\,\mathrm{Ns/m}, \quad k_t = 252\,000\,\mathrm{N/m}.$$

We use the formulation presented in Section 3 to design the static output feedback $H_\infty$ controller via GA [24]. By setting $\alpha = 5$, $\beta = 10$ in Eq. (11) and after 50 generations of evolution,

the obtained controller gain matrix is $K = 10^3 \times [2.2513 \quad 9.8305]$. The closed-loop frequency responses with the above $H_\infty$ controller from disturbance to sprung mass acceleration, suspension deflection and tyre deflection can give a closed-loop which satisfies the three different performance criteria.

Once the desirable damper force is obtained according to the above designed controller, the control of input current to achieve the desirable damper force is determined from Eq. (4), where the desired damper force $F_d$ to be tracked is set by $u(t)$ in Eq. (12), and applied to the MR damper. Due to the actual constraint of the input current to the MR damper, the input current is restricted within $0 \sim 1$ A in this study. The block diagram for the semi-active $H_\infty$ control of vehicle suspension with MR damper is depicted in Fig. 6. It can be seen that the desired damper force is calculated from the designed controller, which is equal to the active control force, then this desired force is approximately realized by the MR damper with an appropriate input current using Eq. (4). Since the input current is calculated in an open-loop formulation, therefore, no additional inner controller is used here as in Ref. [26].

Now, the performance of the designed suspension system under one type of road excitation, i.e. random input, is evaluated through computer simulation. The random input signal, the responses of the suspension system under random excitation with passive, semi-active and active configuration, and the input current to MR damper are shown in Fig. 7, where the velocity of the random input signal is shown in Fig. 7 (a); the responses of the sprung mass acceleration, the suspension deflection, and the tyre deflection are shown in Fig. 7(b)–(d), respectively; Fig. 7(e) shows the desired damper force and the actual MR damper force, and Fig. 7(f) shows the input current to MR damper. In these figures, passive means that the control input $u(t) = 0$ in Eq. (12) for all time, active means that the control input $u(t)$ is realized by Eq. (12), and semi-active means that the control input $u(t)$ (the desired force) is realized by the MR damper with the control structure in Fig. 6. It can be seen from Fig. 7(b)–(d) that both active and semi-active can achieve relatively low magnitude in the time responses of sprung mass acceleration, suspension deflection and tyre suspension, respectively, than that of a passive suspension system. Using the presented control structure in Fig. 6, the semi-active suspension system together with the MR damper can achieve a control performance very similar to an active control except a little deterioration when

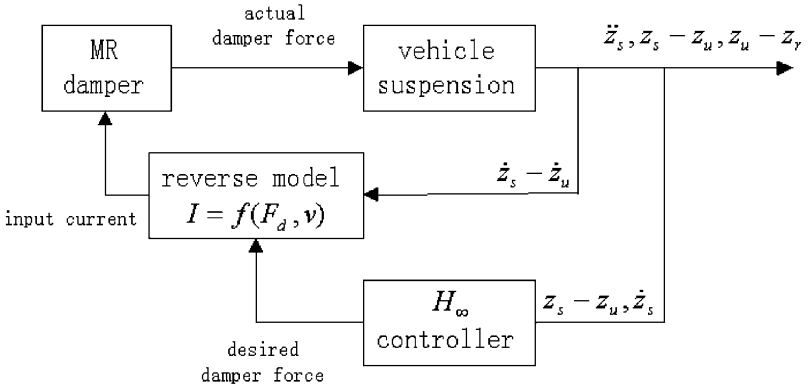


Fig. 6. Block diagram of semi-active $H_\infty$ control for vehicle suspension with MR damper.

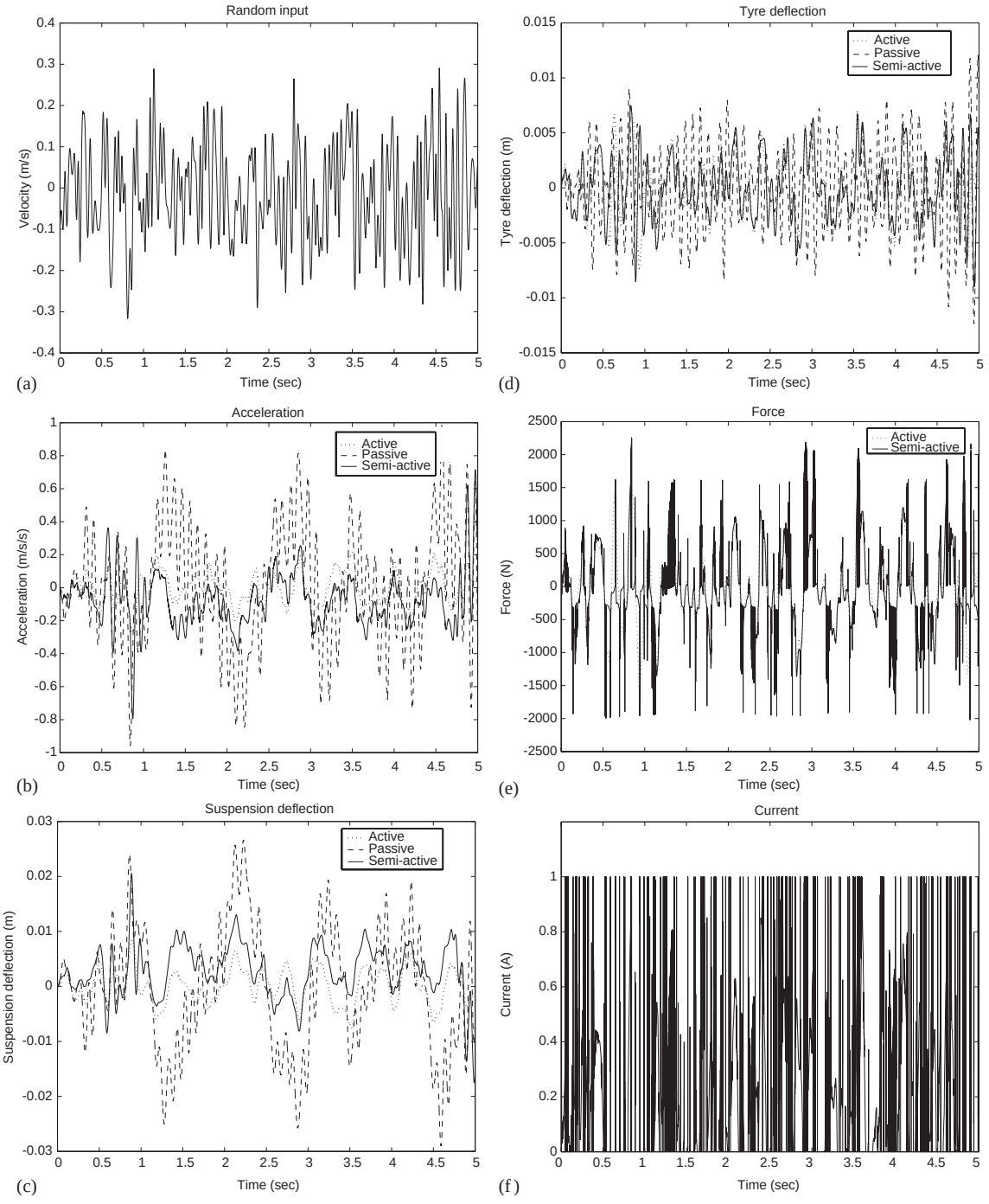


Fig. 7. System responses under random input.

Table 2
RMS analysis for random excitation tests

| Damper | RMS values | | |
|---|---|---|---|
| | Acceleration of sprung mass ($m/s^2$) | Suspension deflection (m) | Tyre deflection (m) |
| Passive | 0.3601 | 0.0112 | 0.0039 |
| Active | 0.0947 | 0.0032 | 0.0028 |
| Semi-active | 0.1035 | 0.0048 | 0.0029 |

the desired force cannot be tracked accurately (as shown in Fig. 7(e)) due to the insufficiency of the polynomial model in describing the MR behavior near the low velocity region and the constraint of the input current to the MR damper (as shown in Fig. 7(f)). It demonstrates the effectiveness of the static output $H_\infty$ controller with MR damper for vibration suppression of the suspension system.

Considering the frequency from 0 to 10 Hz, the root-mean-square (RMS) values of the responses are presented in Table 2. It can also be seen that the active and semi-active suspension systems have good performance in sprung mass acceleration, suspension deflection and tyre deflection than that of passive suspension system; the semi-active suspension with MR damper only has a little degradation of control performance when compared to that of active suspension system. It demonstrates again that the scheme presented in this paper can work well under random excitation.

## 5. Conclusions

The application of MR dampers to semi-active of vehicle suspension is studied in this paper. Together with the polynomial model obtained from the experimental data and a suitably designed static output feedback $H_\infty$ controller, the MR damper is applied to a quarter-car suspension model. The performances of this scheme, validated by numerical simulation, have shown that the static output feedback $H_\infty$ controller combined with the polynomial model of the MR damper can achieve compatible performance as that of active suspension in spite of its simplicity. The polynomial model can characterize the inverse dynamics of the MR damper in analytical form, this allows a static output $H_\infty$ controller be designed directly using the measurable suspension deflection and sprung mass velocity signals. The semi-active $H_\infty$ control scheme developed for vehicle suspension with MR damper can be realized more conveniently in practice. The appropriate selection of MR damper model together with a suitably chosen control strategy will make the application of MR dampers in engineering more successful. Further research works can be done to improve the accuracy of the polynomial model in the low velocity region and more experiments will be done to further test the scheme.

## Acknowledgements

The work was financially supported in part by RGC Grants HKU 7082/97E and 7103/01P. Thanks are extended to Mr. King Ming Chan, Department of Mechanical Engineering, the University of Hong Kong, for helpful preparation of the experiments. The authors are grateful to the reviewers for their helpful comments and valuable suggestions during the revision of this paper.

## References

[1] D. Hrovat, Survey of advanced suspension developments and related optimal control applications, *Automatica* 33 (10) (1997) 1781–1817.
[2] G.Z. Yao, F.F. Yap, G. Chen, W.H. Li, S.H. Yeo, MR damper and its application for semi-active control of vehicle suspension system, *Mechatronics* 12 (7) (2002) 963–973.
[3] C.Y. Lai, W.H. Liao, Vibration control of a suspension system via a magnetorheological fluid damper, *Journal of Vibration and Control* 8 (4) (2002) 527–547.
[4] M. Ahmadian, C.A. Pare, A quarter-car experimental analysis of alternative semiactive control methods, *Journal of Intelligent Material Systems and Structures* 11 (8) (2000) 604–612.
[5] S.B. Choi, H.S. Lee, Y.P. Park, $H_\infty$ control performance of a full-vehicle suspension featuring magnetorheological dampers, *Vehicle System Dynamics* 38 (5) (2002) 341–360.
[6] M. Yokoyama, J.K. Hedrick, S. Toyama, A model following sliding mode controller for semi-active suspension systems with MR dampers, in: *Proceedings of the American Control Conference*, 2001, pp. 2652–2657.
[7] B.F. Spencer Jr., S.J. Dyke, M.K. Sain, J.D. Carlson, Phenomenological model for magnetorheological dampers, *Journal of Engineering Mechanics* 123 (3) (1997) 230–238.
[8] C.C. Chang, P. Roschke, Neural network modeling of a magnetorheological damper, *Journal of Intelligent Material Systems and Structures* 9 (9) (1998) 755–764.
[9] C.C. Chang, L. Zhou, Neural network emulation of inverse dynamics for a magnetorheological damper, *Journal of Structural Engineering* 128 (2) (2002) 231–239.
[10] K.C. Schurter, P.N. Roschke, Fuzzy modeling of a magnetorheological damper using ANFIS, in: *Proceedings of the IEEE International Conference on Fuzzy Systems*, 2000, pp. 122–127.
[11] G. Jin, M.K. Sain, K.D. Pham, B.F. Spencer Jr., J.C. Ramallo, Modeling MR-dampers: a nonlinear blackbox approach, in: *Proceedings of the American Control Conference*, 2001, pp. 429–434.
[12] A. Leva, L. Piroddi, NARX-based technique for the modelling of magneto-rheological damping devices, *Smart Materials and Structures* 11 (1) (2002) 79–88.
[13] N.M. Wereley, L. Pang, G. Kamath, Idealized hysteresis modeling of electrorheological and magnetorheological dampers, *Journal of Intelligent Material Systems and Structures* 9 (8) (1998) 642–649.
[14] S.B. Choi, S.K. Lee, Y.P. Park, A hysteresis model for the field-dependent damping force of a magnetorheological damper, *Journal of Sound and Vibration* 245 (2) (2001) 375–383.
[15] L. Alvarez, R. Jimenez, Real-time indentification of magneto-rheological dampers, in: *Proceedings of 15th IFAC*, 2002, pp. 2252–2258.
[16] Z.G. Ying, W.Q. Zhu, T.T. Soong, A stochastic optimal semi-active control strategy for ER/MR damper, *Journal of Sound and Vibration* 259 (1) (2003) 45–62.
[17] L.M. Jansen, S.J. Dyke, Semiactive control strategies for MR dampers: comparative study, *Journal of Engineering Mechanics* 126 (8) (2000) 795–803.
[18] K.C. Schurter, P.N. Roschke, Neurofuzzy control of structures using magnetorheological dampers, in: *Proceedings of the American Control Conference*, 2001, pp. 1097–1102.
[19] K. Yi, B.S. Song, J.H. Park, Observed-based control of vehicle semi-active suspensions, in: *Proceedings of the Institution of Mechanical Engineers Part D* 213 (1999) 531–543.

[20] J.S. Lin, I. Kanellakopoulos, Nonlinear design of active suspensions, *IEEE Control Systems Magazine* 17 (3) (1997) 45–59.
[21] I. Fialho, G.J. Balas, Design of nonlinear controllers for active vehicle suspensions using parameter-varying control synthesis, *Vehicle System Dynamics* 33 (5) (2000) 351–370.
[22] Y.C. Lin, H.K. Khalil, Two-scale design of active suspension control using acceleration feedback, in: *Proceedings of Conference on Control Applications*, 1992, pp. 884–889.
[23] V.L. Syrmos, C.T. Abdallah, P. Dorato, K. Grigoriadis, Static output feedback—a survey, *Automatica* 33 (2) (1997) 125–137.
[24] H. Du, J. Lam, K.Y. Sze, Non-fragile output feedback $H_\infty$ vehicle suspension control using genetic algorithm, *Engineering Applications of Artificial Intelligence* 16 (8) (2003) 667–680.
[25] P.K.S. Tam, T. Wen, A direct composite $H_\infty$ controller design for a two-time-scale active suspension system, in: *Proceedings of Conference on Industrial Electronics, Control, and Instrumentation*, 1996, pp. 1401–1405.
[26] W.H. Liao, C.Y. Lai, Harmonic analysis of a magnetorheological damper for vibration control, *Smart Materials and Structures* 11 (2) (2002) 288–296.